

## Reduction of parasitic currents in level-set calculations with a consistent discretization of the surface-tension force for the CSF model

R. Meland\*, I.R. Gran, R. Olsen and S.T. Munkejord

SINTEF Energy Research  
 Energy Processes  
 NO-7465 Trondheim, Norway

\*Author for correspondence, E-mail: roarmeland@yahoo.no

### Abstract

Parasitic currents may develop in grid-based interface simulations because of inaccurate representation of the surface forces in the discretized equations. This is due to two causes: firstly, inconsistent discretization of the surface tension force and the pressure gradient, such that the force balance is not fulfilled for a drop or a bubble at rest. Secondly, the problem is inaccurate approximation of the curvature. The least you should demand from a discretization is that it preserves a stationary solution. In this article, it is shown that this can be accomplished by rewriting the interfacial force term in the momentum equation. Using exact curvature, the exact solution for a drop is preserved to machine accuracy. In general, with this discretization, the calculation of the curvature is the only remaining source of spurious currents. Contrary to common practice for the level-set method, we stress that the curvature should be evaluated at the point on the interface whose normal cross the discretization point, and not at the gridpoint in the smeared-out region outside the interface. In 2D, a simple geometrical argument may be used to find the curvature at the interface, whereas in 3D we use extrapolation normal to the interface to create the correct curvature field in a small region around the interface.

### Introduction

Interfacial flows with surface tension are encountered frequently in nature and in industrial processes. Accurate modeling of such flows is challenging due to the discontinuity of material properties across the interface and the need to represent the surface tension forces. The continuum surface force (CSF) method of Brackbill et al. [1] has been employed extensively to model surface tension forces for various fixed grid Cartesian methods where both phases are treated as one field. The surface tension forces acting on the interface are transformed to volume forces in regions near the interface, leading to the ideally discontinuous interfacial jump conditions being modeled as smooth.

For interface methods, calculations often become difficult for fluids with low viscosity when the surface tension force becomes large, i.e. for large curvature. Even in the absence of external forces, e.g. a drop at rest in zero gravity, vortices may appear in the numerical simulation close to an interface, despite the absence of any external forces. These vortices are called spurious or parasitic currents. Parasitic currents have been observed for many interface simulation methods, like the volume-of-fluid (VOF) method, level-set method, and for the front tracking method. The parasitic currents may fail to disappear with mesh refinement, leading to non-convergence of the method. According to Scardovelli and Zaleski [2], the spurious currents become a serious problem when the Laplace number  $La = \sigma\rho r/\mu^2$  is larger than  $10^6$ , which is approximately the value for a 1 cm water drop in air or 1 cm air bubble in water. The parasitic currents develop because of inaccurate represen-

tation of the surface forces in the discretized equations. This is due to two causes: firstly, inconsistent discretization of the surface tension force and the pressure gradient, such that force balance is not fulfilled for a drop or a bubble at rest. Secondly, the problem is inaccurate approximation of the curvature.

Renardy [3] and Francois et al. [4] have shown how to model the surface tension force consistently when used in conjunction with the VOF and the immersed boundary methods. In this article, the same idea is used for the CSF surface tension force in the level-set method.

### Governing equations

In the one field formulation, a single set of continuity and momentum equations are solved on a fixed grid. For two-phase incompressible flow, the equations are

$$\nabla \cdot \mathbf{u} = 0, \quad (1)$$

$$\rho \left( \frac{\partial}{\partial t} \mathbf{u} + \mathbf{u} \cdot \nabla \mathbf{u} \right) = -\nabla p + \nabla \cdot (2\mu \mathbf{D}) + \rho \mathbf{g} - \sigma \kappa \mathbf{n} \delta. \quad (2)$$

Here  $\mathbf{D}$  is the deformation tensor,  $\sigma$  is the surface tension coefficient,  $\kappa$  is the curvature at the interface,  $\mathbf{n}$  is the normal vector at the interface and  $\delta$  is a one-dimensional Dirac delta function with the (signed) distance from the interface as its argument. The momentum equation contains no approximations beyond those in the usual Navier-Stokes equations. This equation is valid for the whole field, even if density and viscosity change discontinuously.

In level-set methods, the interface is represented as the zero level set of a smooth function  $\phi$  representing the distance from the interface, conveniently defined positive on one side of the interface and negative on the other. Using the CSF model, the interface is smeared out over a finite area (2D)/volume (3D) by employing a smeared-out delta function,

$$\mathbf{f}^1 = -\sigma \kappa \mathbf{n} \delta^\epsilon(\phi(\mathbf{r})). \quad (3)$$

The one-dimensional delta function is defined as  $\frac{d}{dx} H(x) = \delta(x)$ . The smeared-out Heaviside function as a function of the signed distance to the interface can be represented as

$$H^\epsilon(\phi) = \begin{cases} 0 & \phi < -\epsilon \\ \frac{1}{2} + \frac{\phi}{2\epsilon} + \frac{1}{2\pi} \sin\left(\frac{\pi\phi}{\epsilon}\right) & -\epsilon \leq \phi \leq \epsilon \\ 1 & \phi > \epsilon \end{cases}$$

and the corresponding smeared-out delta function is

$$\delta^\epsilon(\phi) = \frac{dH^\epsilon}{d\phi} = \begin{cases} 0 & \phi < -\epsilon \\ \frac{1}{2\epsilon} + \frac{1}{2\epsilon} \cos\left(\frac{\pi\phi}{\epsilon}\right) & -\epsilon \leq \phi \leq \epsilon \\ 0 & \phi > \epsilon. \end{cases}$$

Here the width of the smeared region is  $2\epsilon$ , typically  $\epsilon = 1.5\Delta x$  [5].

The curvature and normal vector to the interface that appear in the surface tension term in the momentum equation are calculated from the level-set function. The normal vector is given by

$$\mathbf{n} = \frac{\nabla\phi}{|\nabla\phi|}, \quad (4)$$

and the curvature is defined as

$$\kappa = \nabla \cdot \mathbf{n} = \left( \nabla \cdot \frac{\nabla\phi}{|\nabla\phi|} \right). \quad (5)$$

With the CSF model, the numerical solution becomes continuous at the interface even if the jump conditions imply that the solution should be discontinuous. For example, surface tension forces induce a discontinuous pressure across a fluid-fluid interface, while the methods presented here smear the pressure profile into a numerically continuous function. The density and viscosity are also modelled as continuous functions:

$$\rho(\phi) = \rho^- + (\rho^+ - \rho^-)H^\epsilon(\phi) \quad (6)$$

$$\mu(\phi) = \mu^- + (\mu^+ - \mu^-)H^\epsilon(\phi) \quad (7)$$

where  $\rho^-$ ,  $\mu^-$  are for the fluid with  $\phi < 0$ , and  $\rho^+$ ,  $\mu^+$  are for the fluid with  $\phi > 0$ .

The interfacial movement is determined by the level set advection equation:

$$\frac{\partial\phi}{\partial t} + \mathbf{u} \cdot \nabla\phi = 0.$$

At every time step, the level-set function is reinitialized by a few iterations of the equation

$$\frac{\partial\phi}{\partial\tau} + \mathbf{w} \cdot \nabla\phi = S(\phi_0),$$

where

$$\mathbf{w} = S(\phi_0)\mathbf{n} = S(\phi_0) \frac{\nabla\phi}{|\nabla\phi|} \quad (8)$$

and

$$S(\phi_0) = \frac{\phi_0}{\sqrt{\phi_0^2 + \Delta x^2}}. \quad (9)$$

### Numerical method

The velocity and pressure are decoupled using a projection method [6]. At each time step, the velocities are first integrated as though the pressure term were absent and then a pressure equation is solved to make the velocity divergence free. Let  $\mathbf{u}^n$  be the velocity at time step  $n$ . First, we semi-discretize the momentum equation (2), using forward Euler for the time derivative, and the pressure term is evaluated at step  $n+1$ . Then

$$\mathbf{u}^{n+1} = \mathbf{u}^* - \frac{\Delta t}{\rho} \nabla p^{n+1} \quad (10)$$

where

$$\mathbf{u}^* = \mathbf{u} + \Delta t \left( -\mathbf{u} \cdot \nabla \mathbf{u} + \frac{1}{\rho} \nabla \cdot (2\mu \mathbf{D}) + \mathbf{g} - \frac{1}{\rho} \sigma \kappa \mathbf{n} \delta \right). \quad (11)$$

No superscript means that the terms are evaluated at time step  $n$ . The reason why we use  $p^{n+1}$  instead of  $p^n$ , is that with  $p^n$ ,  $\mathbf{u}^{n+1}$  will not satisfy continuity. Taking the divergence of equation

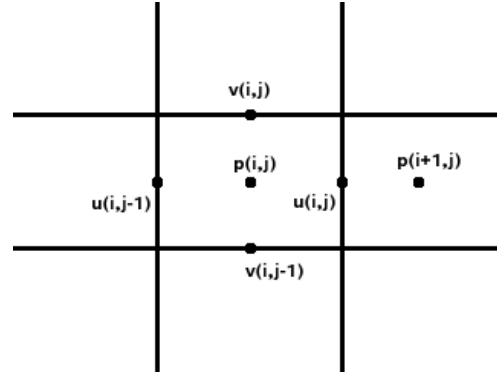


Figure 1: Staggered grid used in the discretization

(10) and stipulating that the new velocity field  $\mathbf{u}^{n+1}$  satisfies the continuity equation, we have

$$\nabla \cdot \left( \frac{1}{\rho} \nabla p^{n+1} \right) = \frac{1}{\Delta t} \nabla \cdot \mathbf{u}^{n*}. \quad (12)$$

The equations are discretized using the finite difference method on a staggered grid. The scalar variables are defined in the center of the cell, and the velocity components are defined at the midpoint of the right and top cell-faces, as indicated in Figure 1. For the convective derivatives, we use WENO [5].

### Balanced force discretization

For zero velocity and no gravity, the one field momentum equation (2) reduces to

$$\nabla p = -\sigma \kappa \nabla I(\mathbf{r}). \quad (13)$$

Here we have used the identity  $\mathbf{n} \delta = \nabla I$ , where  $I$  is the indicator function defined in the following way:

$$I(\mathbf{r}, t) = H(\phi(\mathbf{r})) = \begin{cases} 1, & \phi > 0 \\ 0, & \phi < 0 \end{cases} \quad (14)$$

and  $\mathbf{n}$  is a normal vector at the interface pointing into the phase corresponding to  $\phi > 0$ . For a drop or a bubble with constant surface tension coefficient and curvature, the pressure is given by

$$p = -\sigma \kappa I = -\sigma \kappa H(\phi(\mathbf{r})), \quad (15)$$

i.e. a jump  $\sigma \kappa$  over the interface.

Numerically, the level-set method with the CSF model will not give a sharp interface, but a profile normal to the interface like a smeared Heaviside function. If we use

$$\mathbf{f}^2 = -\sigma \kappa \nabla H^\epsilon(\phi(\mathbf{r})) \quad (16)$$

as the surface tension force, we see that a discrete pressure

$$p_{i,j} = -\sigma \kappa H^\epsilon(\phi(\mathbf{r}_{i,j})) \quad (17)$$

will satisfy the discretized force balance in equation (13), if the same discretization scheme is applied for both  $\nabla H^\epsilon$  and  $\nabla p$ . For example, for the  $x$ -component of equation (13) discretized at the  $u$ -discretization point, we have

$$\frac{p_{i+1,j} - p_{i,j}}{\Delta x} = -\sigma \kappa \frac{H^\epsilon(\phi(\mathbf{r}_{i+1,j})) - H^\epsilon(\phi(\mathbf{r}_{i,j}))}{\Delta x}. \quad (18)$$

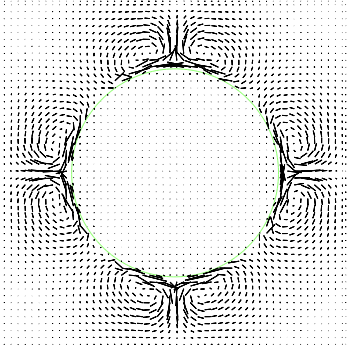


Figure 2: The spurious currents are clearly visible in simulation of water drop at rest

The discretized pressure equation will also be identically satisfied, using ordinary central differencing for all terms

$$\nabla \cdot \left( \frac{1}{\rho} \nabla p^{n+1} \right) = -\sigma \kappa \nabla \cdot \left( \frac{1}{\rho} \nabla H^\varepsilon(\phi(\mathbf{r})) \right). \quad (19)$$

Satisfying discrete force balance for a stationary drop in zero gravity should be a requirement for the discretization, since then one of the sources for the spurious currents is removed. Hence we recommend using

$$\mathbf{f}^2 = -\sigma \kappa \nabla H^\varepsilon(\phi(\mathbf{r})) \quad (20)$$

instead of the usual practice,

$$\mathbf{f}^1 = -\sigma \kappa \mathbf{n} \delta^\varepsilon(\phi(\mathbf{r})) \quad (21)$$

for the surface tension force in the level-set formulation. The surface tension term  $\mathbf{f}^2$  must be included if one or both of the scalar points to the side of the u/v discretization point has  $|\phi| \leq \varepsilon$ .

As a numerical test, we have looked at a water drop with radius  $r = 0.012$  m, viscosity  $\mu_l = 0.001137$  kg/(m s) and density  $\rho_l = 1000$  kg/m<sup>3</sup>, suspended in zero gravity in air with viscosity  $\mu_g = 1.776 \cdot 10^{-5}$  kg/(m s) and density  $\rho_g = 1.226$  kg/m<sup>3</sup>. The surface tension is  $\sigma = 0.0727$  N/m. Since we use a 2D code, we actually simulate the cross section an infinite cylinder. The initial pressure field is given by equation (17). To study spurious currents and not difficulties like mass loss, we do not solve for the level-set function. The water drop is put in the middle of an enclosing box of 4 cm  $\times$  4 cm with no-slip boundary condition at the walls. The system is integrated for 0.1 s on a  $100 \times 100$  grid. With the curvature specified exactly as  $\kappa_0 = -1/r$ , the maximum spurious velocity component is  $1.2 \cdot 10^{-16}$  m/s, corresponding to the round-off error, proving that  $\mathbf{f}^2$  indeed gives a consistent discretization.

However, if  $\mathbf{f}^1 = -\sigma \kappa \mathbf{n} \delta^\varepsilon$  is used, with  $\kappa = \kappa_0$  and with an exact normal vector parallel to the line from the u/v discretization point to the center of the drop, the maximum spurious velocity component is 0.16 m/s at the end of the simulation. A vector plot of the velocity is shown in Figure 2. Hence,  $\mathbf{f}^1$  does not give a consistent discretization, force balance is not fulfilled even though the level-set function, the curvature and the normal vector are given by the exact solution for a static drop.

#### Approximations to the curvature at the interface

To test the relative merits of  $\mathbf{f}^1$  and  $\mathbf{f}^2$  for a drop initially at rest, but with  $p(0) = 0$ , the level set computation included, and

Table 1: Maximum spurious velocity component (m/s)

	25 $\times$ 25	50 $\times$ 50	100 $\times$ 100	200 $\times$ 200
$\mathbf{f}^1$	0.099	0.11	0.13	0.11
$\mathbf{f}^{2a}$	$8.0 \cdot 10^{-3}$	$6.2 \cdot 10^{-3}$	$3.0 \cdot 10^{-3}$	$9.6 \cdot 10^{-4}$
$\mathbf{f}^{2b}$	$1.0 \cdot 10^{-3}$	$4.7 \cdot 10^{-4}$	$1.6 \cdot 10^{-4}$	$4.0 \cdot 10^{-5}$
$\mathbf{f}^{2c}$	$1.6 \cdot 10^{-3}$	$8.9 \cdot 10^{-4}$	$4.7 \cdot 10^{-4}$	$2.4 \cdot 10^{-4}$

with curvature and normal vector given by the level-set function. Otherwise, the settings are the same as before. With the level-set method it is easy to calculate the curvature of any iso-surface of the level-set function. In 2D, equation (5) is equivalent to

$$\kappa = \frac{\phi_{yy}\phi_x^2 - 2\phi_x\phi_y\phi_{xy} + \phi_{xx}\phi_y^2}{(\phi_x^2 + \phi_y^2)^{3/2}}. \quad (22)$$

In the implementations of the level-set method using the CSF model that we have seen, it seems to be standard practice to use the curvature evaluated at the discretization point instead of the curvature at the interface. This will introduce an error, and here we instead try to find the curvature at the point of the interface “corresponding” to the discretization point. In 2D, we can use a simple geometrical argument since the level curves can be viewed locally as parts of concentric circles, and the curvature at the interface is given by

$$\kappa_0 \approx \frac{1}{1/\kappa - \phi}. \quad (23)$$

In 3D this will not work, since then there are two independent principal radii of curvature. What we want is the curvature of the interface extrapolated in the normal direction at both sides of the interface. This can be accomplished in the same manner that the interfacial velocity is extended in the normal direction [5]. For every time step, we calculate the curvature field of the iso-surfaces in a narrow region of the interface. By solving the hyperbolic equation

$$\frac{\partial \kappa_{ex}}{\partial \tau} + S(\phi) \mathbf{n} \cdot \nabla \kappa_{ex} = 0, \quad (24)$$

with  $\kappa_{ex}(\tau = 0) = \kappa$  to steady state, the curvature at the interface is extended in the normal direction, and  $\kappa_{ex}$  is used for the curvature in the surface tension calculation.

In Table 1, the maximum spurious velocity at the end of the simulation is shown for 4 implementations of the surface tension force. In the first row, the result for  $\mathbf{f}^1$  with curvature and normal vector calculated at the discretization point, is shown. The rows below are for  $\mathbf{f}^2$ , but with different curvatures estimates. Case *a* is with curvature calculated at the discretization point, case *b* uses the approximation to the curvature on the interface given by equation (23), and case *c* uses extrapolated curvature given by the solution of equation (24).

Again,  $\mathbf{f}^1$  performs poorly, and there is no improvement as the grid is refined, and hence no convergence with  $\mathbf{f}^1$  for such a high Laplace number. For  $\mathbf{f}^2$ , all curvature estimates gives less spurious currents as the grid is refined. For  $\mathbf{f}^2$ , the mass loss/gain is negligible, but for  $\mathbf{f}^1$ , it is still 1.6% on the finest grid. In Fig. 3, the pressure has been plotted for the cross-section  $y = 0$ . For  $\mathbf{f}^2$ , there is hardly any difference when various curvature estimates are used, so only the solution with curvature estimated as in equation (23) is shown.  $\mathbf{f}^2$  gives the correct pressure jump  $\Delta p = \frac{\sigma}{r} = 6.06$  Pa, and a constant pressure inside the drop, whereas  $\mathbf{f}^1$  does not.

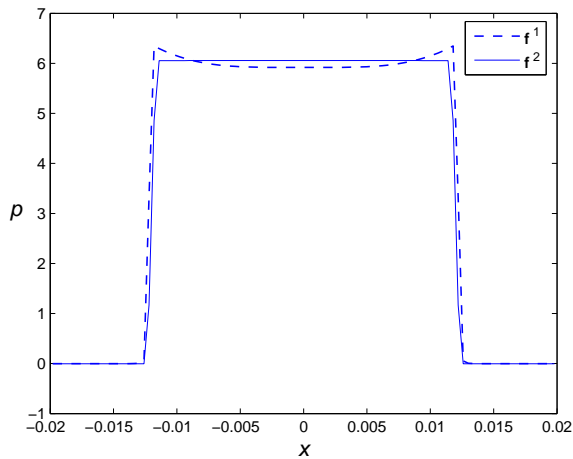


Figure 3: Plot of pressure, cross section through the middle of the drop.  $f^2$  gives the correct pressure jump, and a constant pressure inside the drop, whereas  $f^1$  does not. A  $100 \times 100$  grid has been employed.

Table 2: Area change after 0.05 s for a falling water drop

	$40 \times 60$	$80 \times 120$	$160 \times 240$
$f^1$	7.4%	6.7%	4.4%
$f^{2b}$	0.23%	0.21%	$5.4 \cdot 10^{-2}\%$
$f^{2c}$	0.16%	-0.16%	-0.24%

### Falling drop and rising bubble

First we consider a water drop of radius  $1/300$  m in a  $[-0.01 \text{ m}, 0.01 \text{ m}] \times [-0.02 \text{ m}, 0.01 \text{ m}]$  box filled with air, at ordinary gravity. The drop is released at the origin and the change of area is checked after 0.05 s. The change in area is shown in Table 2, for  $f^1$  with curvature and normal vector calculated at the discretization point, for  $f^{2b}$  with approximation to the curvature on the interface given by equation (23), and for  $f^{2c}$  which uses the extrapolated curvature given by the solution of equation (24).

The results look very encouraging,  $f^{2b}$  give far better mass conservation than  $f^1$ . However, for an air bubble with radius  $1/300$  m released at the origin in a  $[-0.01 \text{ m}, 0.01 \text{ m}] \times [-0.01 \text{ m}, 0.02 \text{ m}]$  box filled with air, there appears to be no improvement using  $\nabla H$  instead of  $\mathbf{n}\delta$  in the surface tension term, as can be seen in Table 3.

### Colliding drops

We consider head-on collision of two 0.75 cm diameter water drops in air, in zero gravity. The drops are released 1.5 cm apart with a velocity  $\pm 0.1$  m/s. The change in area is checked after 0.4 s, then the drops have coalesced and undergone some periods of oscillation. In Table 4, the respective area losses are given for the standard implementation of the CSF surface tension force,  $f^1$ , where curvature and normal vector are calculated

Table 3: Area change after 0.05 s for a rising air bubble

	$40 \times 60$	$80 \times 120$	$160 \times 240$
$f^1$	-8.4%	-3.8%	0.18%
$f^{2b}$	-7.5%	-3.7%	-1.3%
$f^{2c}$	-7.9%	-3.6%	-1.5%

Table 4: Area change for coalescing drops

	$60 \times 60$	$120 \times 120$	$240 \times 240$
$f^1$	30.0%	28.3%	18.4%
$f^{2b}$	-1.2%	0.80%	0.64%

for the iso-surface going through the discretization point, and for  $f^{2b}$ , which is the “balanced force” formulation of the surface tension force, with the curvature evaluated at the interface, using equation (23). Since the Laplace number is high here, it is not unexpected that the standard implementation gives a horrible area loss. However,  $f^{2b}$  gives excellent results.

### Conclusion

The use of a balanced force formulation for the CSF surface tension force together with the curvature evaluated at the interface, seems promising for reducing spurious currents and mass loss in level-set calculations at high Laplace numbers.

### Acknowledgment

This publication forms a part of the Remote Gas project, performed under the strategic Norwegian Research program Petro-maks. The authors acknowledge the partners; Statoil, Hydro, UOP, Aker Kværner, DNV, and the Research Council of Norway (168223/S30) for support.

### References

- [1] Brackbill J.U., Kothe D.B., and Zemach C., A continuum method for modeling surface tension, *Journal of Computational Physics*, Vol. 100, 1992, pp. 335-354
- [2] Scardovelli R., and Zaleski S., Direct numerical simulation of free-surface and interfacial flow, *Annual Review of Fluid Mechanics*, Vol. 31, 1999, pp. 567-603
- [3] Renardy Y., and Renardy M., PROST: A parabolic reconstruction of surface tension for the volume-of-fluid method, *Journal of Computational Physics*, Vol. 183, 2002, pp. 400-421
- [4] Francois M.M., Cummins S.J., Dendy E.D., Kothe D. B., Sicilian J.M., and Williams M.W., A balanced-force algorithm for continuous and sharp interfacial surface tension models within a volume tracking framework, *Journal of Computational Physics*, Vol. 213, 2006, pp. 141-173
- [5] Osher S., and Fedkiw R., *Level-set methods and dynamic implicit surfaces*, Springer, New York, 2003.
- [6] A. J. Chorin, A numerical method for solving incompressible viscous flow problems, *Journal of Computational Physics*, Vol. 2, 1967, pp. 12-26